

## Hadronic production of $S$ - and $P$ -wave states of $\bar{b}c$ -quarkonium

A.V. Berezhnuy, V.V. Kiselev, A.K. Likhoded  
*Theory Division, Institute for High Energy Physics,  
Protvino, Moscow Region, 142284, Russia.*  
*E-mail: likhoded @mx.ihep.su*  
*Fax: +7-095-230 23 37*

### Abstract

In the leading  $O(\alpha_s^4)$  order of the perturbative QCD, the hadronic production cross-sections of  $S$ - and  $P$ -wave states of  $B_c$  meson are calculated. The results for the  $S$ -wave levels are compared with the values given in other papers as well as in the model of the  $b$  quark fragmentation into  $B_c$ . In the given order, the cross-sections of the hadronic production of the  $P$ -wave states are calculated for the first time. Their contribution into the  $B_c$  meson production is less than 10%. There is a strong difference between the predictions of the fragmentation model and the exact perturbative calculations. These differences are discussed in details for the differential distributions over various kinematical quantities.

## Introduction

During recent two years an essential progress has been reached in the understanding of the production mechanisms for the heavy quarkonium, composed of two heavy quarks with different flavours.

The  $\bar{b}c$ -quarkonium production process has the most simple consideration in  $e^+e^-$ -annihilation, where in the limit of high energies ( $M^2/s \ll 1$ ), the differential cross-section has the evident factorizable form

$$\frac{d\sigma_H}{dz} = \sigma_{\bar{b}\bar{b}}(s) \cdot D_{\bar{b} \rightarrow H}(z), \quad (1)$$

where  $z = 2E_{B_c}/\sqrt{s}$ , and  $D_{\bar{b} \rightarrow H}(z)$  is interpreted as the  $\bar{b} \rightarrow H+X$  fragmentation function with  $H$  being the  $\bar{b}c$ -quarkonium [1-3].

Recently, the functions of fragmentation into the  $S$ -,  $P$ -, and  $D$ -wave states for the  $\bar{b}c$ -quarkonium production in  $e^+e^-$  collisions have been found [1-4]. Everywhere below mentioning the fragmentation model we will imply expressions like (1).

The description is more complicated for  $\gamma\gamma$  and hadron-hadron collisions. As for these interactions, in addition to the mechanism of the  $\bar{b}$  quark production with the following fragmentation into the  $\bar{b}c$ -quarkonium, there is a new type of diagrams, corresponding to the photon (gluon) dissociation into the pair of heavy quarks with the following recombination of the quarks into the  $\bar{b}c$ -quarkonium.

In the photon-photon collisions, one can separate three gauge invariant subgroups (6+6+8) within complete set of 20 diagrams in the leading Born approximation, so that subgroups allow one to have the self-consistent interpretations: the  $\bar{b}$  quark fragmentation,

$c$  quark one, and recombination. The contribution of the first mentioned type is quite reliably described by expression (1). For the  $c$  quark fragmentation diagrams one observes a strong deviation from the picture of the fragmentation model. The recombination contribution dominates in the complete region of kinematical variables. As was shown in [5], the given conclusion is valid for the  $S$ -wave state production as well as the  $P$ -wave one [6].

The process of hadronic production of the  $\bar{b}c$ -quarkonium is more difficult for the analysis. In the leading order of the perturbation theory it is described by 36 diagrams in the fourth order over  $\alpha_s$ . At present, there are results of calculations by several groups giving controversial numerical values and conclusions for the  $\bar{b}c$ -quarkonium production cross-sections [7-10]. Moreover, it was offered to simplify the consideration of the heavy quarkonium production by its reduction to the straightforward fragmentation of  $\bar{b}$  quark with the usage of the fragmentation functions, derived for  $e^+e^-$ -annihilation case [11].

In this paper we give the comparative analysis of the results by different papers devoted to the production of the  $S$ -wave states. We prove that the straightforward fragmentation model does not properly describe the  $\bar{b}c$ -quarkonium production. Next, we present the results of calculations for the  $P$ -wave level production over the complete set of the leading order diagrams.

## 1 Calculation technique

The  $A^{SJj_z}$  amplitude of the  $B_c$  meson production can be expressed through the amplitude of four free quarks production  $T^{Ss_z}(p_i, k(\mathbf{q}))$  and the orbital wave function of the  $B_c$  meson,  $\Psi^{Ll_z}(\mathbf{q})$ , in the meson rest frame as

$$A^{SJj_z} = \int T^{Ss_z}(p_i, k(\mathbf{q})) \cdot (\Psi^{Ll_z}(\mathbf{q}))^* \cdot C_{s_z l_z}^{Jj_z} \frac{d^3 \mathbf{q}}{(2\pi)^3}, \quad (2)$$

where  $J$  and  $j_z$  are the total spin of the meson and its projection on  $z$  axis in the  $B_c$  rest frame, correspondingly;  $L$  and  $l_z$  are the orbital momentum and its projection;  $S$  and  $s_z$  are the sum of quark spins and its projection;  $C_{s_z l_z}^{Jj_z}$  are the Clebsh-Gordan coefficients;  $p_i$  are four-momenta of  $B_c$ ,  $b$  and  $\bar{c}$ ,  $\mathbf{q}$  is the three-momentum of  $\bar{b}$  quark in the  $B_c$  meson rest frame;  $k(\mathbf{q})$  is the four-momentum, obtained from the four-momentum  $(0, \mathbf{q})$  by the Lorentz transformation from the  $B_c$  rest frame to the system, where the calculation of  $T^{Ss_z}(p_i, k(\mathbf{q}))$  is performed. Then, the four-momenta of  $\bar{b}$  and  $c$  quarks, composing the  $B_c$  meson, will be determined by the following formulae with the accuracy up to  $|\mathbf{q}|^2$  terms

$$\begin{aligned} p_{\bar{b}} &= \frac{m_b}{M} P_{B_c} + k(\mathbf{q}), \\ p_c &= \frac{m_c}{M} P_{B_c} - k(\mathbf{q}), \end{aligned} \quad (3)$$

where  $m_b$  and  $m_c$  are the quark masses,  $M = m_b + m_c$ , and  $P_{B_c}$  is the  $B_c$  momentum. Let us note that for the  $P$ -wave states it is enough to take into account only terms, linear over  $\mathbf{q}$  in eq.(2), and  $\mathbf{q} = 0$  in the  $S$ -wave production.

The product of spinors  $v_{\bar{b}} \bar{u}_c$ , corresponding to the  $\bar{b}$  and  $c$  quarks in the  $T^{Ss_z}(p_i, k(\mathbf{q}))$  amplitude of eq.(2), should be substituted by the projection operator

$$\mathcal{P}(\Gamma) = \sqrt{M} \left( \frac{\frac{m_b}{M} \hat{P}_{B_c} + \hat{k} - m_b}{2m_b} \right) \Gamma \left( \frac{\frac{m_c}{M} \hat{P}_{B_c} - \hat{k} + m_c}{2m_c} \right), \quad (4)$$

where  $\Gamma = \gamma^5$  for  $S = 0$ , or  $\Gamma = \hat{\varepsilon}^*(P_{B_c}, s_z)$  for  $S = 1$ , where  $\varepsilon(P_{B_c}, s_z)$  is the polarization vector for the spin-triplet state.

For the sake of convenience, one can express the  $\mathcal{P}(\Gamma)$  operator through the spinors of the following form

$$\begin{aligned} v'_b(p_b + k, \pm) &= \left(1 - \frac{\hat{k}}{2m_b}\right) v_b(p_b, \pm), \\ u'_c(p_c - k, \pm) &= \left(1 - \frac{\hat{k}}{2m_c}\right) u_c(p_c, \pm), \end{aligned} \quad (5)$$

where  $v_b(p_b, \pm)$  and  $u_c(p_c, \pm)$  are the spinors with the given projection of quark spin on  $z$  axis in the  $B_c$  meson rest frame. Note, that the spinors in eq.(5) satisfy the Dirac equation for the antiquark with the momentum  $p_b + k$  and mass  $m_b$  or for the quark with the momentum  $p_c - k$  and mass  $m_c$  up to the linear order over  $k$  ( i.e. over  $\mathbf{q}$ , too), correspondingly.

One can easily show that the following equalities take place

$$\begin{aligned} \sqrt{\frac{2M}{2m_b 2m_c}} \frac{1}{\sqrt{2}} \{v'_b(p_b + k, +)\bar{u}'_c(p_c - k, +) - v'_b(p_b + k, -)\bar{u}'_c(p_c - k, -)\} &= \\ &= \mathcal{P}(\gamma^5) + O(k^2), \\ \sqrt{\frac{2M}{2m_b 2m_c}} v'_b(p_b + k, +)\bar{u}'_c(p_c - k, -) &= \\ &= \mathcal{P}(\hat{\varepsilon}^*(P, -1)) + O(k^2), \\ \sqrt{\frac{2M}{2m_b 2m_c}} \frac{1}{\sqrt{2}} \{v'_b(p_b + k, +)\bar{u}'_c(p_c - k, +) + v'_b(p_b + k, -)\bar{u}'_c(p_c - k, -)\} &= \\ &= \mathcal{P}(\hat{\varepsilon}^*(P, 0)) + O(k^2), \\ \sqrt{\frac{2M}{2m_b 2m_c}} v'_b(p_b + k, -)\bar{u}'_c(p_c - k, +) &= \\ &= \mathcal{P}(\hat{\varepsilon}^*(P, +1)) + O(k^2). \end{aligned} \quad (6)$$

In the  $B_c$  rest frame, the polarization vectors of the spin-triplet state have the form

$$\begin{aligned} \varepsilon^{rf}(-1) &= \frac{1}{\sqrt{2}}(0, 1, -i, 0), \\ \varepsilon^{rf}(0) &= (0, 0, 0, 1), \\ \varepsilon^{rf}(+1) &= -\frac{1}{\sqrt{2}}(0, 1, i, 0). \end{aligned} \quad (7)$$

In calculations the Dirac representation of  $\gamma$ -matrices is used and the following explicit form of the spinors is applied

$$\begin{aligned} u(p, +) &= \frac{1}{\sqrt{E+m}} \begin{pmatrix} E+m \\ 0 \\ p_z \\ p_x + ip_y \end{pmatrix}, & u(p, -) &= \frac{1}{\sqrt{E+m}} \begin{pmatrix} 0 \\ E+m \\ p_x - ip_y \\ -p_z \end{pmatrix} \\ v(p, +) &= -\frac{1}{\sqrt{E+m}} \begin{pmatrix} p_z \\ p_x + ip_y \\ 0 \\ E+m \end{pmatrix}, & v(p, -) &= \frac{1}{\sqrt{E+m}} \begin{pmatrix} p_x - ip_y \\ p_z \\ 0 \\ E+m \end{pmatrix} \end{aligned} \quad (8)$$

The  $S$ -wave production amplitude can be written down as

$$A^{Ss_z} = iR_S(0) \sqrt{\frac{2M}{2m_b 2m_c}} \sqrt{\frac{1}{4\pi}} \left( T^{Ss_z}(p_i, k(\mathbf{q} = 0)) \right), \quad (9)$$

where  $R_S(0)$  is the radial wave function at the origin, so that

$$R_S(0) = \sqrt{\frac{\pi}{3}} \tilde{f}_{B_c},$$

and the  $\tilde{f}_{B_c}$  value is related with the leptonic constants of pseudoscalar and vector  $B_c$  states

$$\begin{aligned} \langle 0 | J_\mu(0) | V \rangle &= i f_V M_V \epsilon_\mu, \\ \langle 0 | J_{5\mu}(0) | P \rangle &= i f_P p_\mu, \end{aligned}$$

where  $J_\mu(x)$  and  $J_{5\mu}(x)$  are the vector and axial-vector currents of the constituent quarks. Then the account for hard gluon corrections in the first order over  $\alpha_s$  [12] results in

$$\tilde{f} = f_V \left[ 1 - \frac{\alpha_s^H}{\pi} \left( \frac{m_2 - m_1}{m_2 + m_1} \ln \frac{m_2}{m_1} - \frac{8}{3} \right) \right], \quad (10)$$

$$\tilde{f} = f_P \left[ 1 - \frac{\alpha_s^H}{\pi} \left( \frac{m_2 - m_1}{m_2 + m_1} \ln \frac{m_2}{m_1} - 2 \right) \right], \quad (11)$$

where  $m_{1,2}$  are the masses of quarks, composing the quarkonium. For the vector currents of quarks with equal masses, the BLM procedure of the scale fixing in the "running" coupling constant of QCD [13] gives (see paper by M.B.Voloshin in ref.[12])

$$\alpha_s^H = \alpha_s^{\overline{\text{MS}}}(e^{-11/12} m_Q^2).$$

The estimates of the  $\tilde{f}_{B_c}$  value within the potential models have the essential uncertainty,  $\tilde{f}_{B_c} = 500 \pm 100$  MeV [14]. The QCD sum rule estimate of the  $f_{B_c}$  value for the pseudoscalar state gives  $f_{B_c} = 385 \pm 25$  MeV [15], which is in a good agreement with the evaluation in the framework of recent lattice computations [16], where  $f_{B_c} = 395(2)$  MeV with the error bar, giving the statistical uncertainty only. The  $\tilde{f}_{B_c}$  estimate strongly depends on the  $\alpha_s^H$  scale choice, which is not yet calculated in the BLM procedure. So, we use  $\tilde{f}_{B_c} = 570$  MeV.

For the  $P$ -wave states in eq.(2), the  $T^{Ss_z}(p_i, k(\mathbf{q}))$  amplitude can be expanded into the Taylor series up to the terms linear over  $\mathbf{q}$ . Then one gets

$$A^{Sjz} = i R'_P(0) \sqrt{\frac{2M}{2m_b 2m_c}} \sqrt{\frac{3}{4\pi}} C_{s_z l_z}^{jz} \mathcal{L}^{l_z} \left( T^{Ss_z}(p_i, k(\mathbf{q})) \right), \quad (12)$$

where  $R'_P(0)$  is the first derivative of the radial wave function at the origin, and  $\mathcal{L}^{l_z}$  has the following form

$$\begin{aligned} \mathcal{L}^{-1} &= \frac{1}{\sqrt{2}} \left( \frac{\partial}{\partial q_x} + i \frac{\partial}{\partial q_y} \right), \\ \mathcal{L}^0 &= \frac{\partial}{\partial q_z}, \\ \mathcal{L}^{+1} &= -\frac{1}{\sqrt{2}} \left( \frac{\partial}{\partial q_x} - i \frac{\partial}{\partial q_y} \right), \end{aligned} \quad (13)$$

where  $\frac{\partial}{\partial q_x}$ ,  $\frac{\partial}{\partial q_y}$ ,  $\frac{\partial}{\partial q_z}$  are the differential operators acting on  $T^{Ss_z}(p_i, k(\mathbf{q}))$  as the function of  $\mathbf{q} = (q_x, q_y, q_z)$  at  $\mathbf{q} = 0$ .

As all considered matrix elements are calculated in the system distinct from the  $B_c$  rest frame, the four-momentum  $k(\mathbf{q})$  has been calculated by the following formulae

$$\begin{aligned} k^0 &= \frac{\mathbf{v} \cdot \mathbf{q}}{\sqrt{1-\mathbf{v}^2}}, \\ \mathbf{k} &= \mathbf{q} + \left( \frac{1}{\sqrt{1-\mathbf{v}^2}} - 1 \right) \frac{\mathbf{v} \cdot \mathbf{q}}{\mathbf{v}^2} \mathbf{v}, \end{aligned} \quad (14)$$

where  $\mathbf{v}$  is the  $B_c$  velocity in the system, where the calculations are performed. The matrix element  $T^{Ssz}(p_i, k(\mathbf{q}))$  is computed, so that the four-momenta of  $\bar{b}$  and  $c$  quarks are determined by eq.(3), taking into account eq.(14).

The first derivatives in eq.(13) are substituted by the following approximations

$$\frac{\partial T^{Ssz}(p_i, k(\mathbf{q}))}{\partial q_j} \Big|_{\mathbf{q}=\mathbf{0}} \approx \frac{T^{Ssz}(p_i, k(\mathbf{q}^j)) - T^{Ssz}(p_i, 0)}{\Delta}, \quad (15)$$

where  $\Delta$  is some small value, and  $\mathbf{q}^j$  have the following form

$$\begin{aligned} \mathbf{q}^x &= (\Delta, 0, 0), \\ \mathbf{q}^y &= (0, \Delta, 0), \\ \mathbf{q}^z &= (0, 0, \Delta). \end{aligned} \quad (16)$$

With the chosen values of quark masses and interaction energies, the increment value  $\Delta = 10^{-5}$  GeV has provided the stability of 4-5 meaning digits in the squared matrix elements summed over  $j_z$  for all  $P$ -wave states with the given value of  $J$  and  $S$ , when one has performed the Lorentz transformations along the beam axis or the rotation around the same axis.

One has to note that because of such transformations, the new vectors  $k(\mathbf{q}^j)$  do not correspond to the transformed old vectors. Therefore, the applied test is not only a check of the correct typing of the  $T^{Ssz}(p_i, k(\mathbf{q}))$  amplitude, but it is also the check of correct choice of the phases in eq.(12).

The matrix element  $A^{SJj_z}$  squared, which is calculated by the method described above, must be summed over  $j_z$  as well as the spin states of free  $b$  and  $\bar{c}$  quarks. It also must be averaged over spin projections of initial particles.

The phase space integration has been made by the Monte Carlo method of RAMBO program [11].

## 2 $S$ -wave states

Let us consider the calculation results for the  $gg$ -production of the  $S$ -wave  $\bar{b}c$ -quarkonium levels ( $B_c$  and  $B_c^*$ ) in comparison with the values given in other papers. The cross-section of the process under consideration is proportional to the  $\tilde{f}_{B_c}$  squared as well as to the fourth power of  $\alpha_s$ . To compare the results of different papers, we rescale all the numbers to the values, determined by the same set of  $\alpha_s = 0.2$  and  $\tilde{f}_{B_c} = 570$  MeV, which are used in the given calculations. We also fix the mass values of  $m_b = 4.8$  GeV and  $m_c = 1.5$  GeV.

The cross-sections of the gluonic production of  $B_c^{(*)}$  versus the total energy of the  $gg$  collisions are presented in Fig. 1. In addition to the results of the complete numerical

calculations of the  $O(\alpha_s^4)$  contribution, we give also the values, obtained in the fragmentation model and, hence, calculated as the product of the  $gg$ -production cross-section for the  $b\bar{b}$ -pair and the probability of the  $\bar{b} \rightarrow B_c^{(*)}$  fragmentation, calculated at the same set of parameters.

As one can see in this figure, there is a good agreement of our previous calculations [7] with the results of refs.[8,10]. The values, given in two other papers of ref.[9], are approximately three times greater than our results. In this paper we have recalculated the cross-sections in the axial gauge, used in ref.[9], in contrast to the covariant Feynman gauge applied in our previous consideration [7]. The corresponding numerical results have not changed after the replacement of the gauge. This fact points to errors in the computations, performed in ref.[9].

In the studied region of energies, the ratio of the  $B_c$  and  $B_c^*$  yields,  $R = \sigma_{B_c^*}/\sigma_{B_c} \simeq 3$ , strongly deviates from  $R \simeq 1.4$  predicted by the fragmentation model. One can also see in Fig. 1, that in the region of the applicability determined by the condition  $M^2/s \ll 1$ , the fragmentation model gives the total cross-section, which is essentially smaller than the exact result evaluated over the complete set of diagrams.

As one can see in Fig. 2, the total cross-section of the  $B_c^{(*)}$  production is basically accumulated in the region of the transverse momenta close to  $p_T \sim M_{B_c}$ . One could expect, that the fragmentation mechanism begins to dominate at large  $p_T$ . Indeed, the  $p_T$ -distribution shown in Fig. 2 for  $B_c$  and  $B_c^*$  at  $\sqrt{s} = 100$  GeV, points to the fact, that there is a quite good coincidence of the distribution tails obtained from exact perturbative calculations and in the fragmentation model. Numerically, this agreement takes place at  $p_t > 40$  GeV for  $B_c$ . Thus, one can draw the certain conclusion, that the fragmentation contribution is not dominant in the  $gg$ -collisions. It also does not describe the distribution over the variable defined as  $z = 2|\vec{P}_{B_c}|/\sqrt{s}$ . This fact is evident in Fig. 3. At  $z$  values close to unit, the fragmentation model overestimates the exact perturbative result.

To get the cross-section and  $p_T$  spectra in hadron-hadron collisions, one should convert the partonic  $gg$  cross-section with the distribution functions of gluons in the initial hadrons. We use the parametrization of ref.[17] for the parton distributions at the fixed virtuality scale  $Q = 2m_b \sim 10$  GeV. In the framework of the given approximation, we fix also the coupling constant value  $\alpha_s = 0.2$ .

The convolution result is presented in Fig. 4 for the energy of the FNAL Tevatron ( $\sqrt{s} = 1.8$  TeV). The histograms correspond to the exact perturbative results, whereas the curves are calculated according to the following formula

$$\begin{aligned} \frac{d\sigma}{dp_T} \quad ( \quad \bar{p}p \rightarrow H_{(p_T)}x ) &= \sum_{i,j} \int dx_1 dx_2 dz f_{i/p}(x_1, \mu) f_{j/\bar{p}}(x_2, \mu) \times \\ &\times \frac{d\hat{\sigma}}{dp_T} \quad ( \quad ij \rightarrow \bar{b}(p_T/z) + x ) \times D_{\bar{b} \rightarrow H}(z, \mu), \end{aligned} \quad (17)$$

where  $D(z, \mu)$  is the function of the  $\bar{b} \rightarrow H$  fragmentation with  $H = B_c, B_c^*, \dots$ ,  $d\hat{\sigma}/dp_T$  is the differential cross-section of the  $\bar{b}$  quark production, and  $f_{i/A}(x, \mu)$  is the distribution of the  $i$ -kind parton in the  $A$ -hadron.

As one can see in the figure, the curves certainly deviate from the histograms of the exact perturbative calculations in the all region of  $p_T$ . At small  $p_T$ , the fragmentation model gives the overestimation, whereas at large  $p_T$ , contrary, it underestimates the exact

result. It is significant to note the fact, that the perturbative calculations and the model give the different values for the ratio of the differential cross-sections of  $B_c^*$  and  $B_c$ . One finds the yield ratio  $R \sim 2 \div 3$ , whereas the model gives  $R \sim 1.3 \div 1.5$ .

The qualitative agreement between the model and perturbative calculations for the  $d\sigma/dp_T$  distribution of  $B_c$  meson has allowed the authors of ref.[8] to conclude on the satisfactory description of the exact perturbative  $O(\alpha_s^4)$ -contribution by the fragmentation model. The misleading is related to the fact, that those values of the  $gg$ -collision energy are included in the integration region of expression (17), where the approximation of the fragmentation does not work or it is not strictly defined, i.e., where the  $M^2/s \ll 1$  condition is evidently not valid. As one can see in Fig. 1 at these low energies, the cross-section in the fragmentation model and that of the perturbative result have the different dependency on the energy. The latter fact is because of the use of the two-particle phase space in the fragmentation approximation of the heavy quark production instead of the real three-particle phase space ( $B_c$ ,  $\bar{b}$  and  $c$  are in the final state).

To avoid the uncertainties related with the low energy of  $gg$ -collisions, we have started the integration over  $\hat{s}$  in expression (17) from  $\sqrt{\hat{s}} > 60$  GeV. As one can see in Fig. 5, the given cut drastically changes the relation between the fragmentation model contribution and the exact perturbative result. It indicates that the fragmentation model can not provide an adequate approximation for the correct description of the hadronic  $B_c$  meson production.

One has to note, that the given conclusion does not depend on the definite choice of the structure functions for the initial hadrons as well as on a special modification of the fragmentation expression.

Thus, the conclusion drawn in ref.[8] about the dominance of the fragmentation mechanism in the hadronic production of  $B_c$  mesons, is incorrect.

### 3 Production of $P$ -wave states

As it was mentioned above, to get the cross-section for the production of the  $P$ -wave quarkonium levels it is necessary to calculate the first derivative of the quark production matrix element over  $\vec{q}$ , the relative momentum of the quarks inside the  $B_c$  meson. This procedure of calculations has been tested by comparison of the numerical computation of the fragmentation functions for the  $\bar{b}$  quark into the  $P$ -wave states with known analytical expressions for the corresponding functions obtained in ref.[4]. We have found a good agreement between the  $^1P_1$ ,  $^3P_0$ ,  $^3P_1$ , and  $^3P_2$ -level cross-sections calculated numerically, and those obtained from the analytical expressions for the same set of parameters,  $m_b$ ,  $m_c$ ,  $|R'_P(0)|^2$  and  $\alpha_s$ . The total cross-sections of the gluonic production of  $P$ -wave levels are presented versus the total energy of the collisions in Tab. 1. The dependence of the cross-section, summed over the spin states of the  $P$ -levels, on the energy of the interacting gluons is shown in Fig. 6. This dependence can be approximately described by the following expression

$$\sigma_{B_c(L=1)} = 25 \cdot \left(1 - \left(\frac{2(m_b + m_c)}{\sqrt{s}}\right)\right)^{1.95} \cdot \left(\frac{2(m_b + m_c)}{\sqrt{s}}\right)^{1.2} \text{ pb.} \quad (18)$$

The contribution, determined by the fragmentation model, is also shown in the same figure, where it is found as the corresponding total  $gg \rightarrow b\bar{b}$  cross-section multiplied by

the integral probability of the  $b \rightarrow B_c(L = 1)$  fragmentation,  $W = 5.34 \cdot 10^{-5}$ . The  $c$ -quark fragmentation is suppressed by the order of magnitude in the hadron collisions, and we will neglect it below.

As one can see in Fig. 6, the total cross-section of the  $P$ -wave level production is much greater than the value predicted by the fragmentation model, which has a strict meaning in the region of high energies, and, thereby, the contribution of the recombination diagrams dominates. The fragmentation contribution also does not describe the  $d\sigma/dz$  distributions, which are the differential cross-sections integrated over the transverse momentum of  $P$ -wave levels. These distributions are shown in Fig. 7. It is interesting to notice that in contrast to the  $\gamma\gamma$ -collisions, the result of the fragmentation model essentially overestimates the exact perturbative values in the gluonic collisions. This fact, related with the interference of different contributions, will be discussed elsewhere.

The distributions over the transverse momentum of the produced  $P$ -wave states are presented in Fig. 8 in comparison with the results of the fragmentation model. One can see, that the fragmentation is valid only on the tails. This fact is quite expected, since the same picture has been observed in the production of  $S$ -levels.

Thus, our calculations of the  $P$ -wave level production cross-sections show that the total hadronic cross-sections are about 10% of the corresponding cross-sections of the  $S$ -wave levels, and the recombination mechanism dominates for the both  $S$ - and  $P$ -levels.

The differential distributions for the  $P$ -wave states calculated by convoluting the partonic cross-sections with the gluon distributions, as it was described in previous Section, are shown in Fig. 9 for the FNAL Tevatron energy,  $\sqrt{s} = 1.8$  TeV.

As it comes for the  $S$ -wave states, the calculation over formula (1) of the fragmentation model gives a rather approximate qualitative value for the  $P$ -level cross-section. The reason of such "description" is generally related to the uncertainty of the fragmentation approach in the region of energies close to the kinematical threshold of the reaction, where the fragmentation model overestimates the cross-section. This incorrect contribution compensates the underestimation in the region of large energies and small or moderate  $p_T$ , where the recombination dominates. This results in the approximate description of the exact perturbative distribution by the fragmentation formula at  $p_T \sim 15$  GeV (see Fig. 9). As it was shown in previous Section, the  $\hat{s}$  cut clarifies the problem, and one evidently conclude, that the exact perturbative calculations and the fragmentation model strongly differ in the predictions.

## Conclusion

Let us analyse the results of the numerical perturbative calculations performed for the hadronic production cross-sections of the  $S$ - and  $P$ -wave levels of the  $\bar{b}c$ -quarkonium in the leading  $O(\alpha_s^4)$  order of the perturbative QCD.

There are two scales of virtualities in the problem. The first one is of the order of the heavy quark masses, and it appears in the heavy quark production. The second scale is determined by the characteristic relative momentum of the quarks inside the  $\bar{b}c$ -meson. Since the latter is much less than the masses of the produced quarks, the process of the  $B_c$  production can be separated into two steps:

- 1) the heavy quark production, described in the perturbative QCD, and

2) the forming of the bound state, described by the quarkonium wave function at the origin.

The results, hence, linearly depend on  $\alpha_s^4$ ,  $\tilde{f}_{B_c}^2$  and  $|R'_P(0)|^2$ . Moreover, there are the additional parameters defining the quark masses,  $m_b$  and  $m_c$ . The bulk of the uncertainty of the results is connected with the  $\alpha_s$ ,  $\tilde{f}_{B_c}$ , and  $|R'_P(0)|$  values. For instance, the use of the running coupling constant  $\alpha_s(\hat{s})$  instead of  $\alpha_s(4m_b^2)$  as well as the use of a smaller value of  $\tilde{f}_{B_c}$  can decrease the cross-section by order of magnitude.

From our point of view, the use of  $\alpha_s(\hat{s})$  is not correct, since the analysis shows that typical virtualities in the production of four heavy quarks are less than  $\hat{s}$  at large  $\hat{s}$ . This is why we have fixed the value of  $\alpha_s = 0.2$ . The comparison with the results of other papers shows, that we agree with the calculations of the  $S$ -level production in ref.[8], but, in contrast to [8], we compare the yields of pseudoscalar and vector states of  $B_c$  in the hadronic production to emphasize the invalidity of the fragmentation model to the problem under consideration. The results of ref.[9] disagree with the values given in our paper for both total cross-section of the pseudoscalar state and the dependence on the total energy. The production of the vector state was not considered in ref.[9]. So, our computations, performed in covariant and axial gauges, point to errors in papers of ref.[9].

The exact perturbative cross-sections for the  $P$ -wave states are found for the first time. As well as for the hadronic production of  $S$ -levels, one observes the strong discrepancy in the values of the relative yields of  $^1P_1$ ,  $^3P_0$ ,  $^3P_1$  and  $^3P_2$ -levels in comparison with the production in  $e^+e^-$ -annihilation. This fact points to the different dominating mechanisms. The fragmentation of the  $\bar{b}$  quark into  $B_c^{(*)}$  is the basic mechanism in  $e^+e^-$ -annihilation, whereas the recombination of heavy quarks dominates in the hadronic production of  $B_c^{(*)}$ .

## Acknowledgements

A.K. Likhoded thanks E. Eichten and C. Quigg for fruitfull discussions and stimulating remarks.

This work is supported, in part, by the Russian Foundation of Fundametal Researches. The work of A.V. Berezhnoy has been made possible by a fellowship of INTAS Grant 93-2492 and one of International Soros Science Education Program Grant A1377 and it is carried out within the research program of International Center for Fundamental Physics in Moscow.

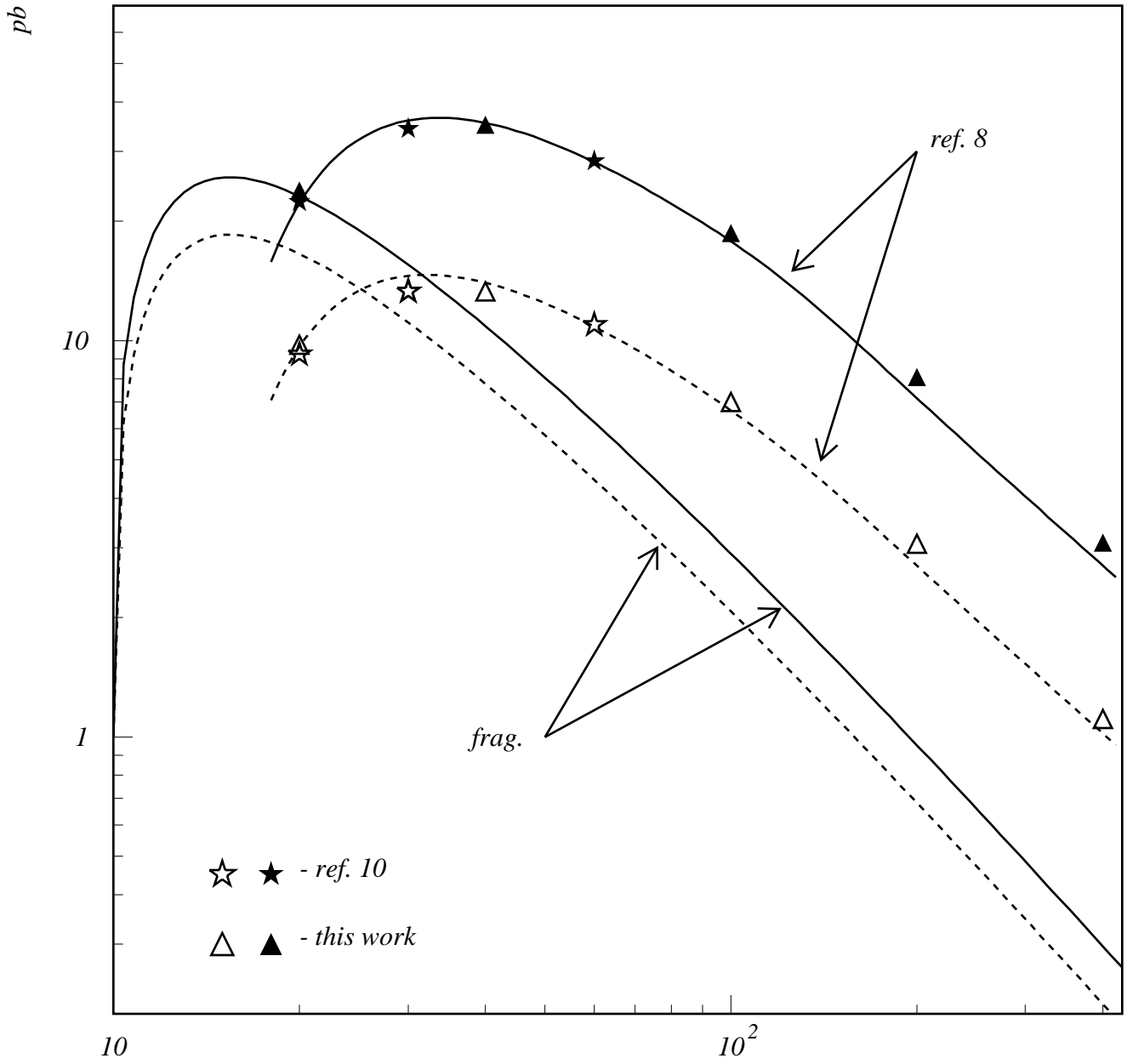
## References

1. L. Clavelli, Phys. Rev. D26 (1982) 1610;  
C.-R. Ji and R. Amiri, Phys. Rev. D35 (1987) 3318;  
C.-H. Chang and Y.-Q. Chen, Phys. Lett. B284 (1992) 127.
2. E. Braaten, K. Cheung, T.C. Yuan, Phys. Rev. D48 (1993) 4230.
3. V.V. Kiselev, A.K. Likhoded, M.V. Shevlyagin, Z. Phys. C63 (1994) 77.
4. T.C. Yuan, Phys. Rev. D50 (1994) 5664;  
K. Cheung, T.C. Yuan, Preprint UCD-95-24, 1995.
5. A.V. Berezhnoy, A.K. Likhoded, M.V. Shevlyagin, Phys. Lett. B342 (1995) 351;  
K. Kołodziej, A. Leike, R. Rückl, Phys. Lett. B348 (1995) 219.
6. A.V. Berezhnoy, V.V. Kiselev, A.K. Likhoded, Preprint IHEP 95-119, Protvino, 1995 [hep-ph/9510238].
7. A.V. Berezhnoy, A.K. Likhoded, M.V. Shevlyagin, Yad. Fiz. 58 (1995) 730;  
A.V. Berezhnoy, A.K. Likhoded, O.P. Yushchenko, Preprint IHEP 95-59, Protvino, 1995 [hep-ph/9504302].
8. K. Kołodziej, A. Leike, R. Rückl, Phys. Lett. B355 (1995) 337.
9. M. Masetti, F. Sartogo, Phys. Lett. B357 (1995) 659;  
S.R. Slabospitsky, Preprint IHEP 94-53, Protvino, 1994 [hep-ph/9404346].
10. C.-H. Chang, Y.-Q. Chen, G.-P. Han and H.-Q. Jiang, Phys. Lett. B364 (1995) 78.
11. K. Cheung, T.C. Yuan, Preprint NUHEP-TH-94-20, 1994.
12. M.B. Voloshin, M.A. Shifman, Sov. J. Nucl. Phys. 47 (1988) 511;  
E. Braaten, S. Fleming, Phys. Rev. D52 (1995) 181;  
M.B. Voloshin, Int. J. Mod. Phys. A10 (1995) 2865;  
V.V. Kiselev, Preprint IHEP 95-63, Protvino, 1995 [hep-ph/9504313], to appear in Int. J. Mod. Phys. A.
13. S.J. Brodsky, G.P. Lepage, P.B. Mackenzie, Phys. Rev. D28 (1983) 228.
14. S.S. Gershtein et al., Uspekhi Fiz. Nauk 165 (1995) 3, Phys. Rev. D51 (1995) 3613;  
E. Eichten and C. Quigg, Phys. Rev. D49 (1994) 5845.
15. S. Narison, Phys. Lett. B210 (1988) 238;  
V.V. Kiselev, A.V. Tkabladze, Sov. J. Nucl. Phys. 50 (1989) 1063);  
T.M. Aliev, O. Yilmaz, Nuovo Cimento 105A (1992) 827;  
P. Colangelo, G. Nardulli, N. Paver, Z. Phys. C57 (1993) 43;  
C.A. Dominguez, K. Schilcher, Y.L. Wu, Phys. Lett. B298 (1993) 190;  
S. Reinshagen, R. Rückl, Preprints CERN-TH.6879/93 and MPI-Ph/93-88, 1993;  
E. Bagan et al., Z. Phys. C64 (1994) 57;  
M. Chabab, Phys. Lett. B325 (1994) 205.

16. S. Kim, Preprint SNU-TP-95-088, hep-lat/9511010, 1995.
17. J.Botts et al., CTEQ Coll., Preprint ISU-NP-92-17, MSUHEP-92-27 (1992).

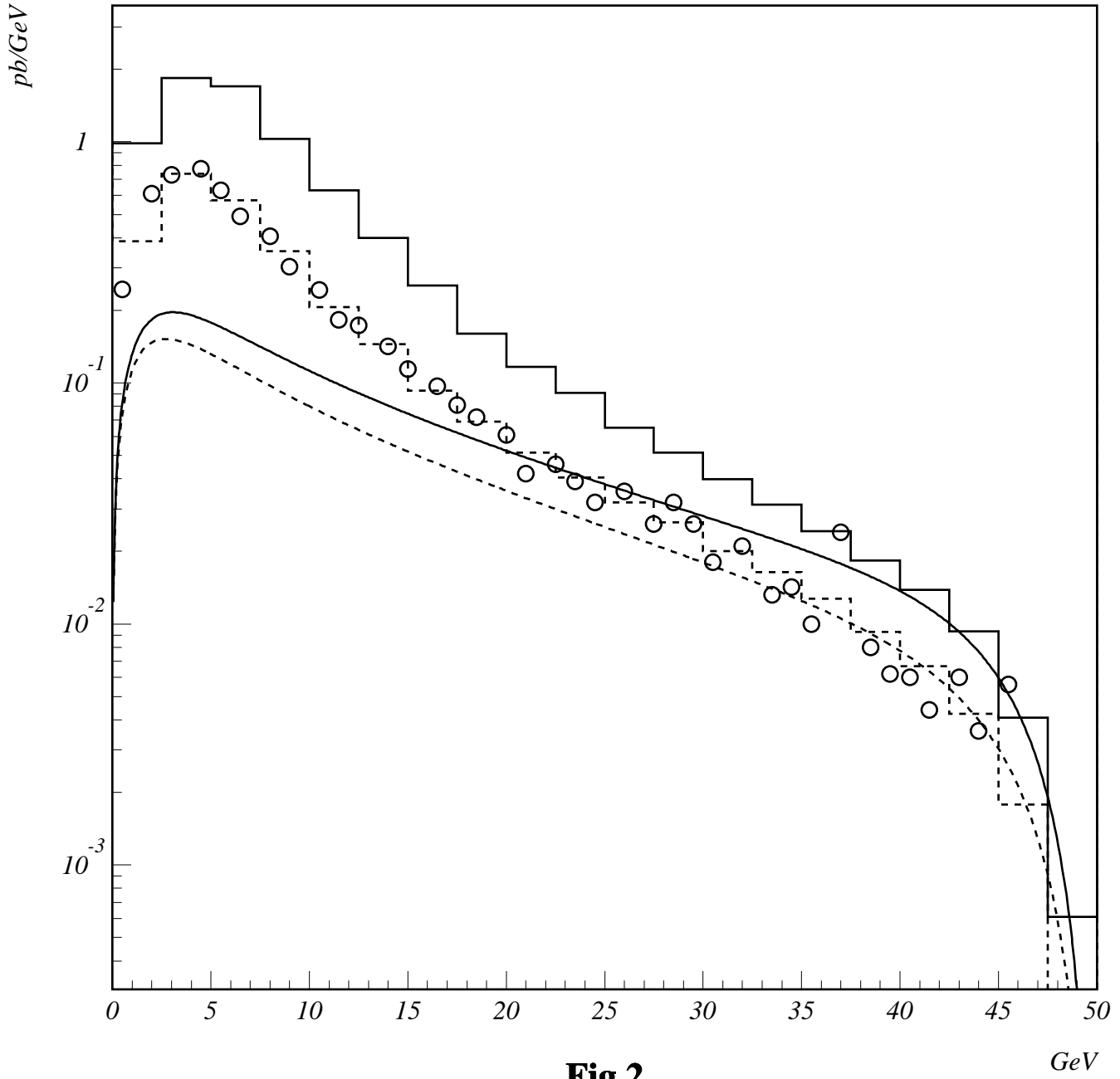
## Figure captions

- Fig. 1. The total cross-section of the gluon-gluon production of  $B_c$  (empty triangle) and  $B_c^*$  (solid triangle) in comparison with the predictions of the fragmentation model (frag.) and the results of ref.[8] (curves) and ref.[10] (stars).
- Fig. 2.  $d\sigma/dp_T$  at  $\sqrt{\hat{s}} = 100$  GeV for  $B_c^*$  (solid histogram) and  $B_c$  (dashed histogram) in comparison with the predictions of the fragmentation model (solid and dashed curves for  $B_c^*$  and  $B_c$ , respectively), and the result of ref.[8] for  $B_c$  (dots).
- Fig. 3.  $d\sigma/dz$  at  $\sqrt{\hat{s}} = 100$  GeV for  $B_c^*$  (solid histogram) and  $B_c$  (dashed histogram) in comparison with the predictions of the fragmentation model (curves).
- Fig. 4.  $d\sigma/dp_T$  in the hadronic production of  $B_c^*$  (solid histogram) and  $B_c$  (dashed histogram) in comparison with the predictions of the fragmentation model (curves) at the  $p\bar{p}$ -collision energy  $\sqrt{s} = 1.8$  TeV.
- Fig. 5. The same as in Fig. 4 with the  $\sqrt{\hat{s}} > 60$  GeV cut off.
- Fig. 6. The total cross-section summed over spins of the  $P$ -levels in the gluon-gluon production (dots) and its fit (solid line curve) in comparison with the prediction of the fragmentation model (dashed line curve).
- Fig. 7.  $d\sigma/dz$  at  $\sqrt{\hat{s}} = 100$  GeV for  $^1P_{1-}$ ,  $^3P_{0-}$ ,  $^3P_{1-}$ , and  $^3P_{2-}$ -levels (a, b, c and d figures, correspondingly) in comparison with the predictions of the fragmentation model (curves).
- Fig. 8.  $d\sigma/dp_T$  with the same notations as in Fig. 7.
- Fig. 9. The differential cross-section of the hadronic  $p\bar{p}$  production of the  $P$ -level  $B_c$  mesons at  $\sqrt{s} = 1.8$  TeV (histograms) in comparison with the fragmentation model results:  $^3P_{2-}$  solid curve,  $^3P_{0-}$  dotted curve,  $^3P_{1-}$  dash-dotted curve, and  $^1P_{1-}$  dashed curve.



**Fig.1**

GeV



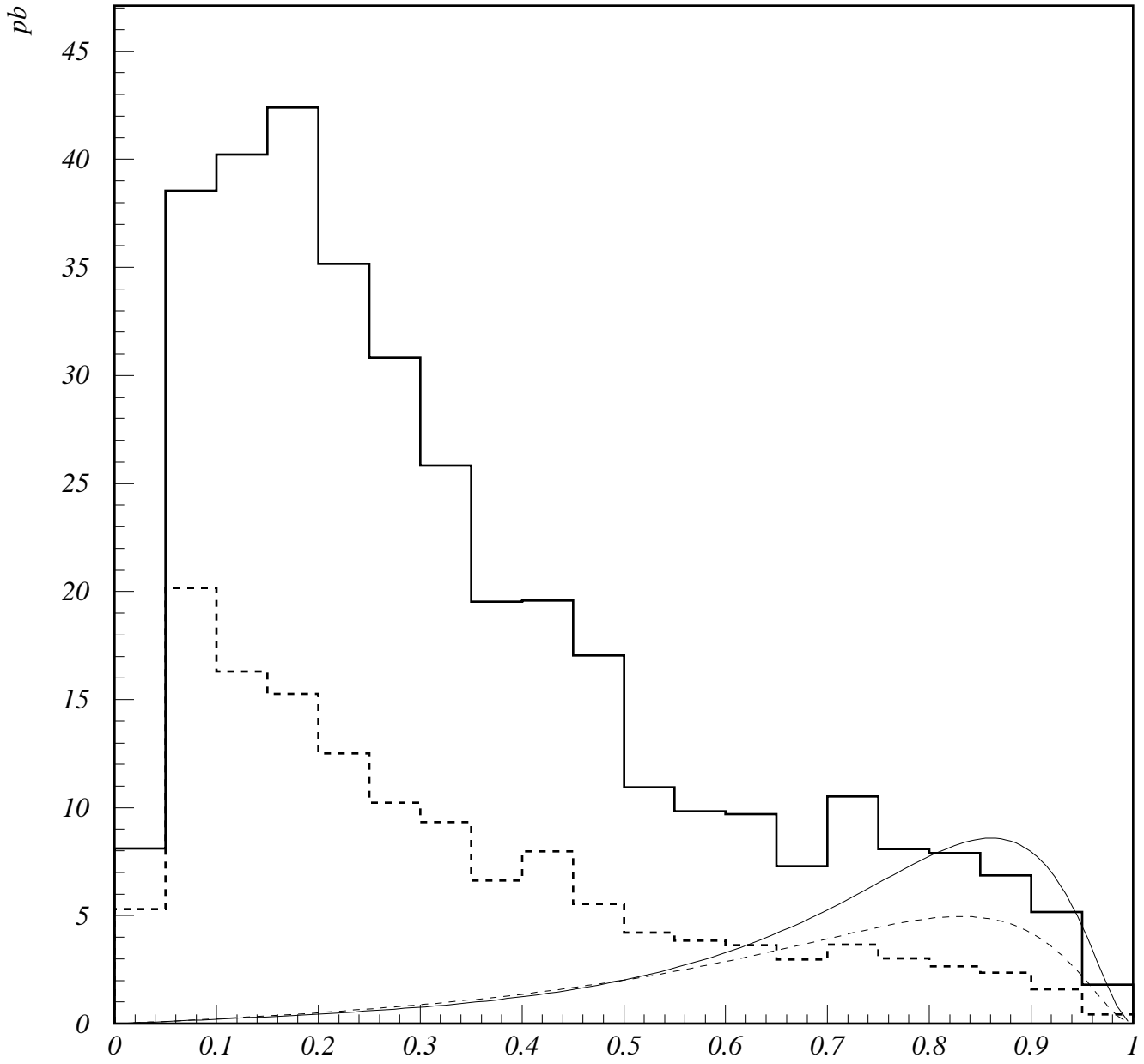


**Fig.3**

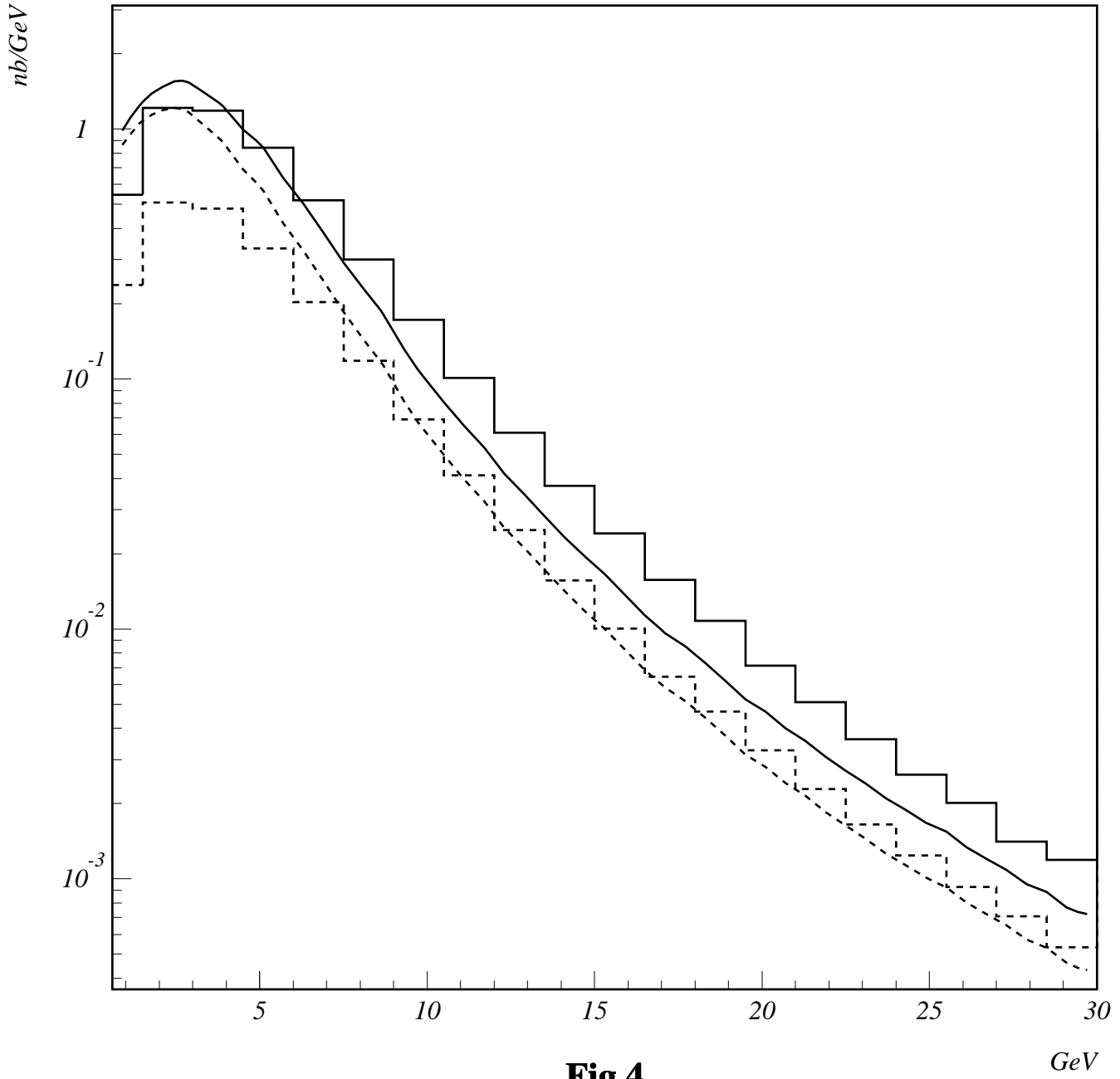


**Fig.4**

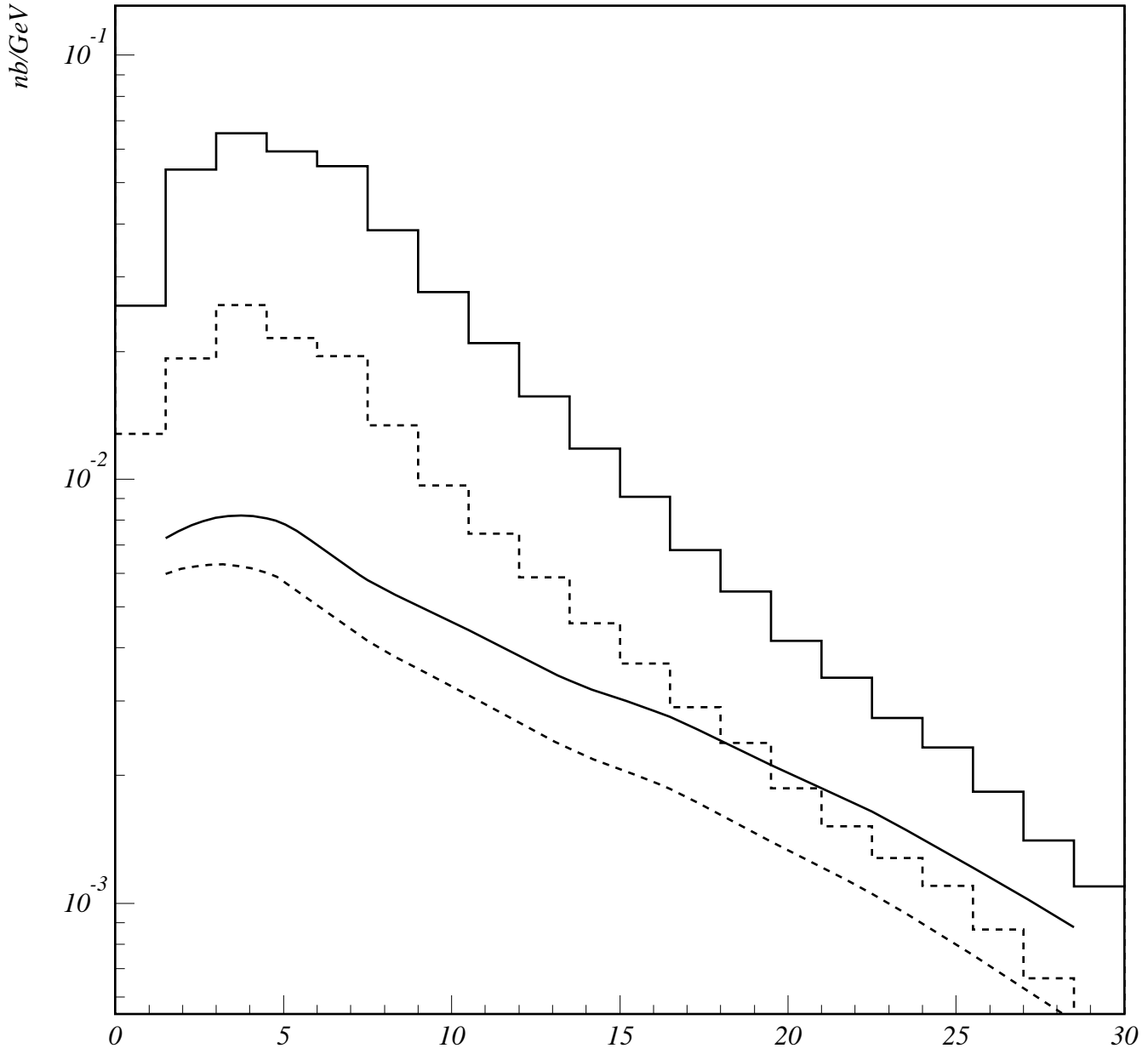


**Fig.5**

*GeV*

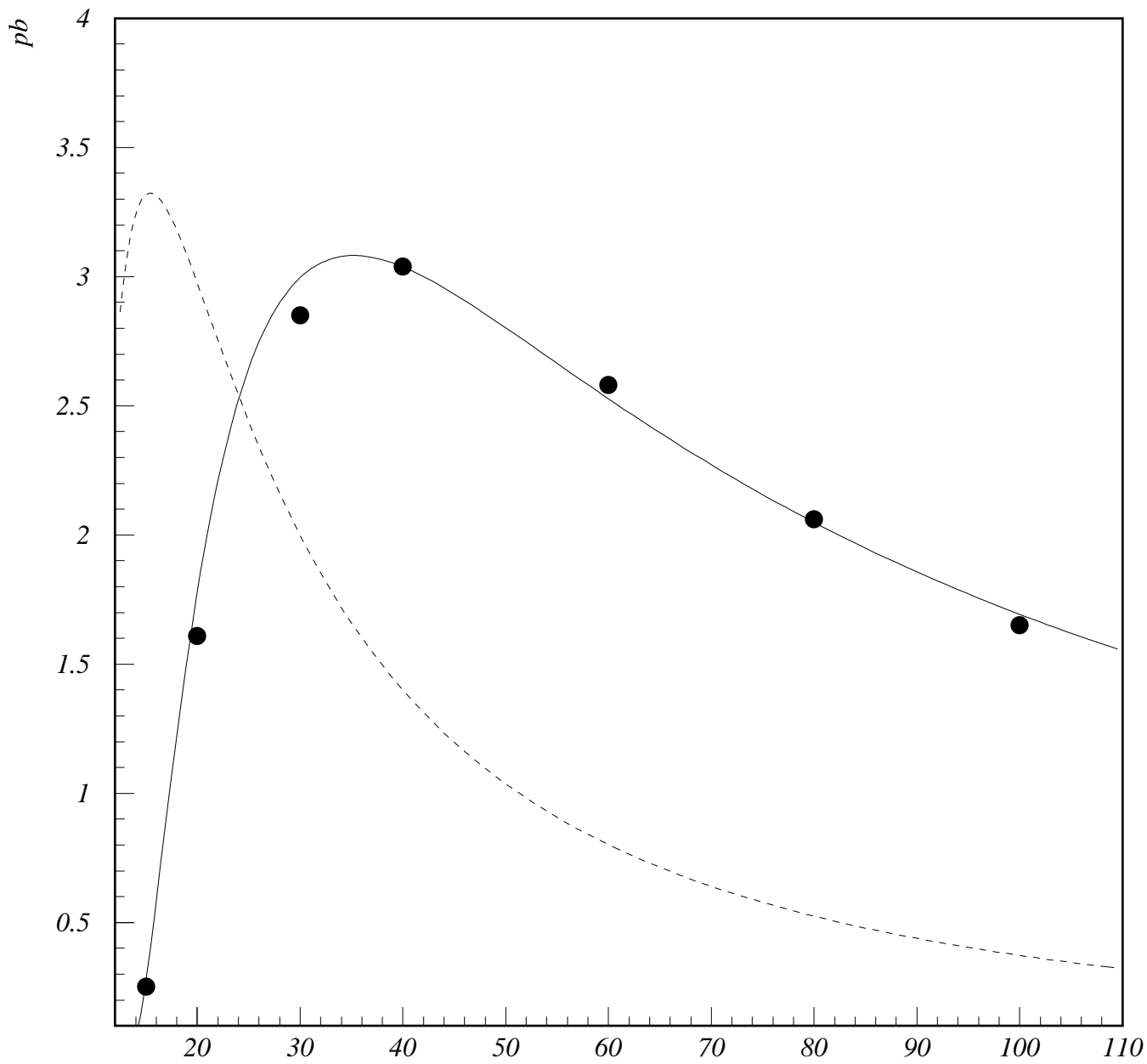


**Fig.6**

GeV

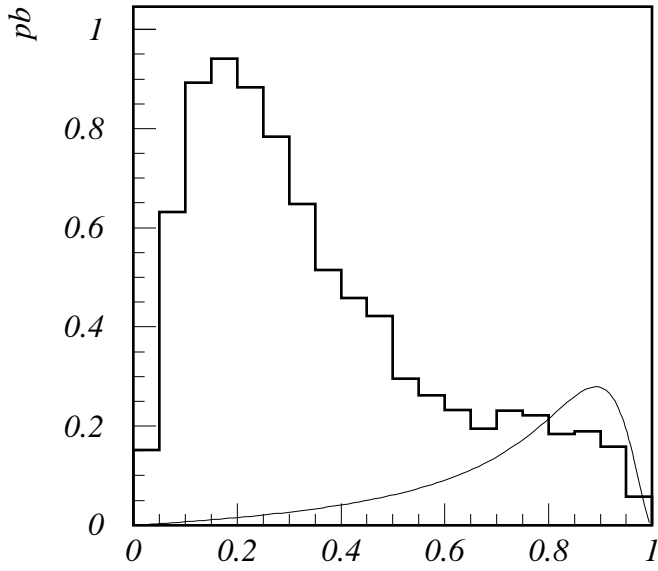


**Fig.7a**

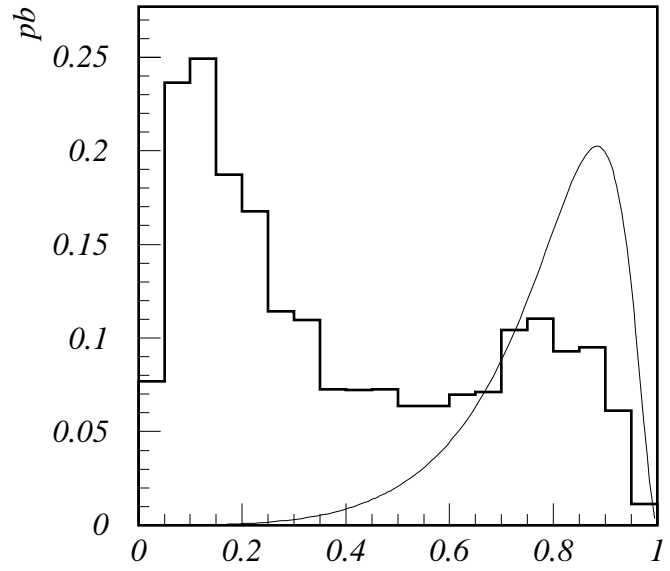


**Fig.7b**

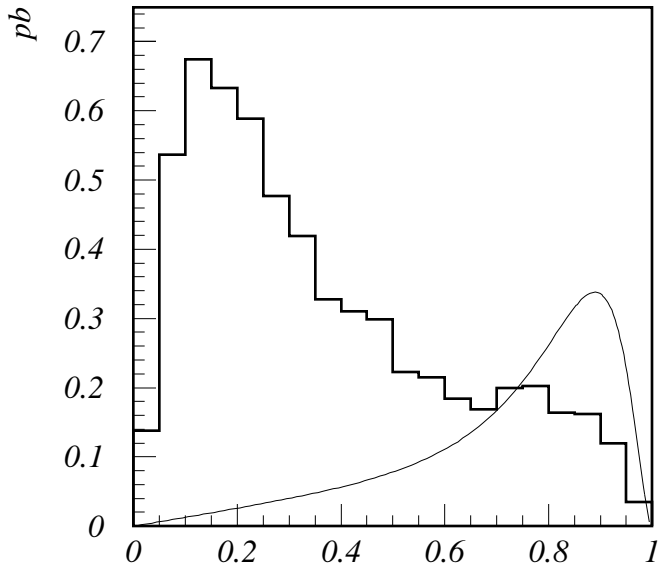


**Fig.7c**

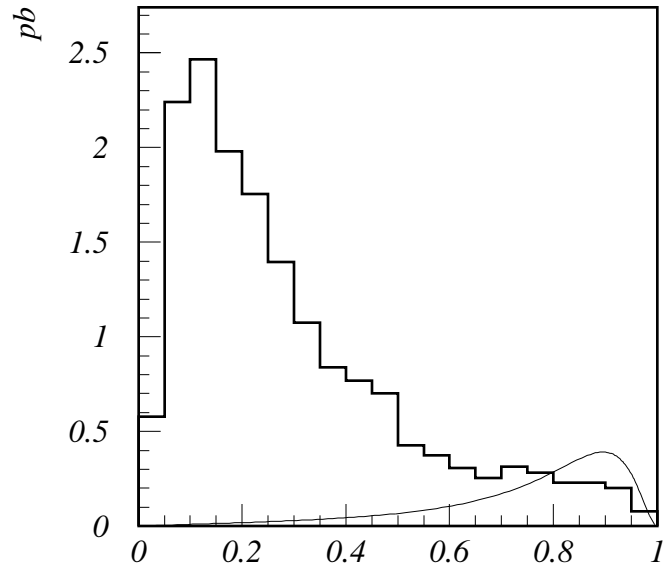


**Fig.7d**

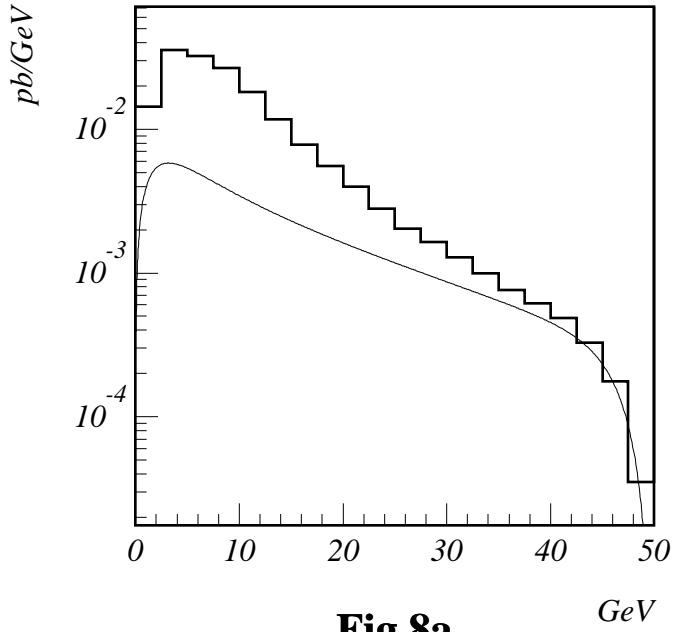


**Fig.8a**

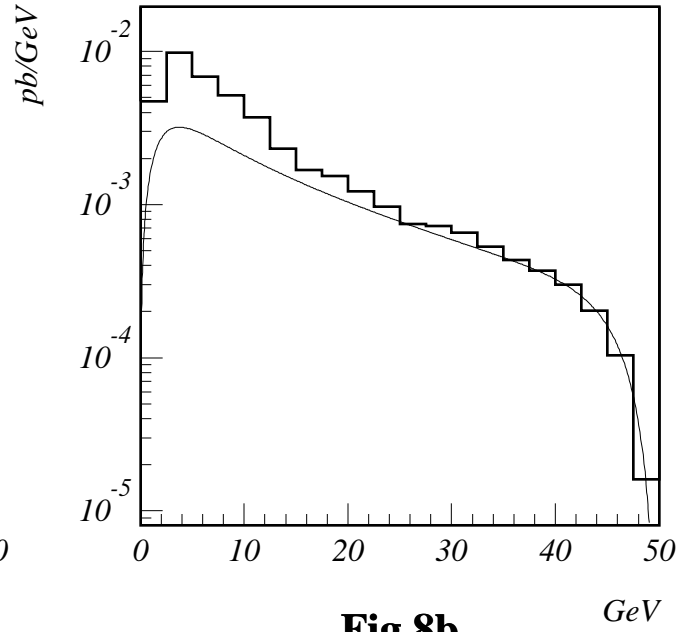


**Fig.8b**

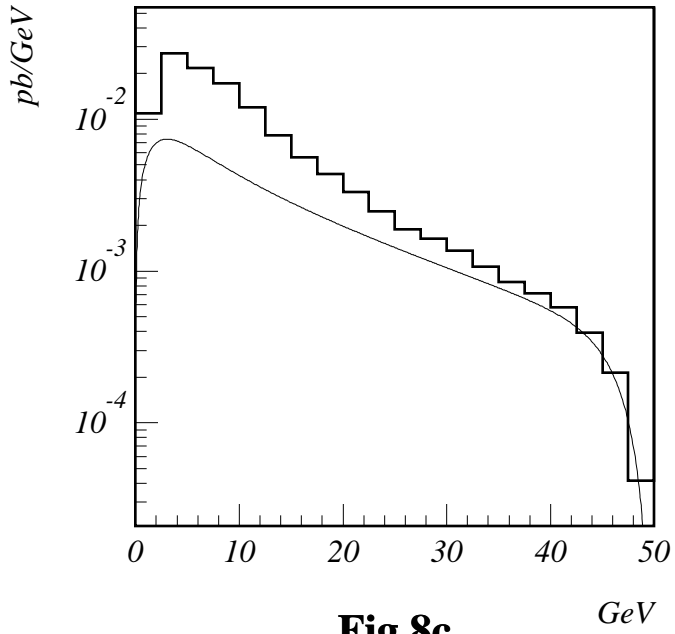


**Fig.8c**

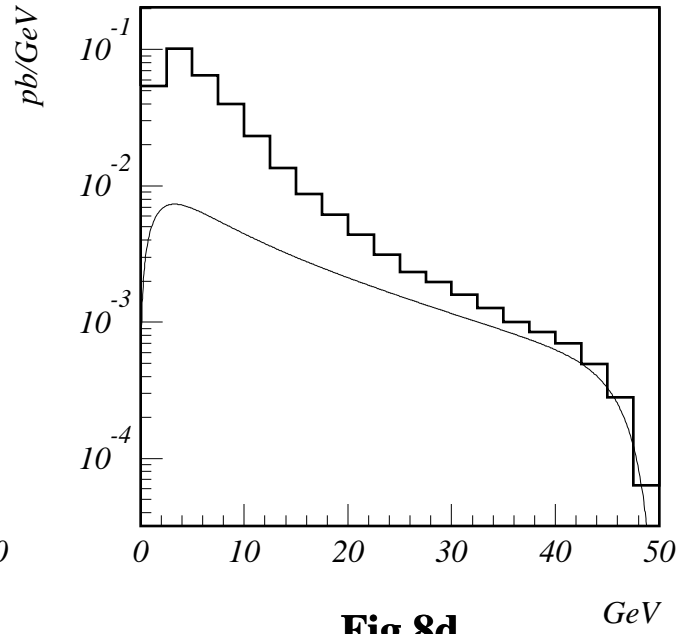


**Fig.8d**

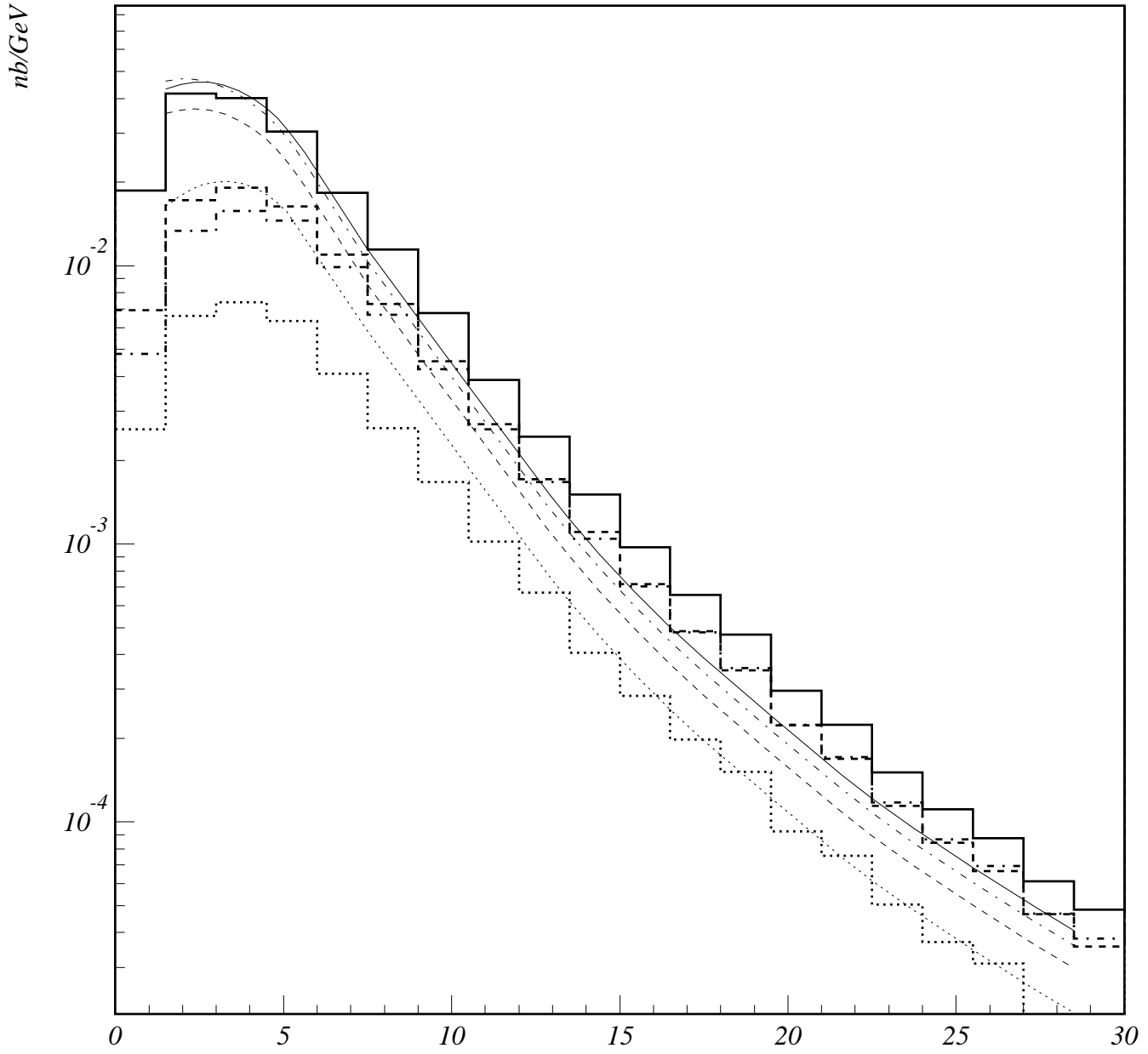


**Fig.9**

*GeV*